THE KICKER MAGNET FOR THE FAST EJECTION SYSTEM OF THE SERPUKHOV 70 GeV PROTON ACCELERATOR

E. Frick, B. Kuiper, A. Messina, H. Riege
CERN, Geneva, Switzerland

Abstract

This full aperture magnet produces a field of 0.1 T with a rise-time of 150 nsec in an aperture of 140 x 100 mm^2 and over a magnetic length of 3 m. It is a two-section L-C network incorporated in a delay line pulser circuit. Its construction and performance are described.

I. Introduction

The delay line magnet principle of O'Neill[1] has found wide application for inflectors and ejectors of high energy particle accelerators. A number of circuits and constructions, adapted to the application in question, have been made or are being proposed[2]. The performance specifications of the Serpukhov kicker magnet[3] were more severe than hitherto encountered and a great flexibility, like supplied for the old CPS system[4], was required for the planned three-shot operation into three interlaced ejection channels. A new assessment has therefore been made of a number of magnet types and constructions, in particular in view of the low impedance of 5 Ω to be used. It has been published at this conference in 1970[5]. The assessment used computations and full scale prototype studies.

One main point of interest is the pulse performance, i.e. rise time, fall time, flat top and spurious field after the main pulse. The rise time τ_o of a matched distributed delay line magnet excited with a step-pulse is known to be:

$$\tau_o = \sqrt{L_o \cdot C} = L_o/R \qquad (1)$$

where L_o is the magnet inductance, ideally given by the gap geometry and magnetic length, i.e. including azimuthal leakage fields as far as contributing to the kick. C is the capacitance and R the characteristic impedance. The practical rise time t_r is longer than τ_o, due to further leakage fields, stray inductances and non-zero rise time of the excitation pulse. This may be expressed as

$$t_r = x \cdot \tau_o = x \cdot L_o/R \qquad (2)$$

where the downgrading factor $x > 1$ accounts globally for all mentioned effects. The pulse voltage V required for excitation of a kick (field integral) K over an aperture width w in a rise time t_r then becomes

$$V = \frac{K \cdot w}{N \cdot \tau_o} = x \frac{K \cdot w}{N \cdot t_r}, \qquad (3)$$

where N is the number of modules into which the magnet is divided. A downgrading factor $x \sim 1.3$ could be achieved. This value, the conventional formulae[2,6] and expressions (2) and (3) then yield the systems parameters of Table I.

TABLE I. Design Parameters of Janus Kicker Magnet

	Symbol	Unit	Value
Total length of magnetic circuit	ℓ	m	3.0
Total magnetic length, including leakage fields contributing to kick	ℓ_m	m	3.25
Gap height	h	m	0.10
Gap width	w	m	0.14
Number of modules	N		10
Total kick	K	T.m	0.3
Magnetic field	B	T	0.1
Rise time (0-100 %)	t_r	nsec	150
Downgrading factor	x		1.3
Time constant = L_o/R	τ_o	nsec	114
Fall time (100-10 %)	t_f	nsec	135
Reflections (w.r.t. proton bunches)	ΔK_o	%	$< \pm$ 10
Ripple flat top "	ΔK_t	%	$< \pm$ 3
Kick inhomogeneity	ΔK_r	%	$< \pm$ 3
Excitation current	I	kA	8
Line circuit impedance	Z_o	Ω	5
Pulse voltage	V	kV	40
Line charging voltage	V_o	kV	80
Pulse duration	T_p	μs	0.17-5.1
Geometric gap inductance (using magnetic length)	L_o	μH	0.57
Capacitances	C1	nF	12
	C2	nF	11
Magnetic stored energy = $\frac{1}{2} L_o I^2$	W_m	J	~17
Electric stored energy = $\frac{1}{2} (C1 + C2) V^2$	W_e	J	~18

II. The System[7]

The 3 meter long kicker magnet is divided in 10 modules which are incorporated into 10 independently powered delay line pulser circuits (Fig. 1). The modules are grouped in pairs with antisymmetrical excitation loops. Powering "left" and "right" modules of each pair with pulses of opposite polarity produces therefore the same polarity field. For this the pulse generators are also grouped in pairs and charged with relevant polarities. This makes the system compatible with addition of a mechanical field inverter,

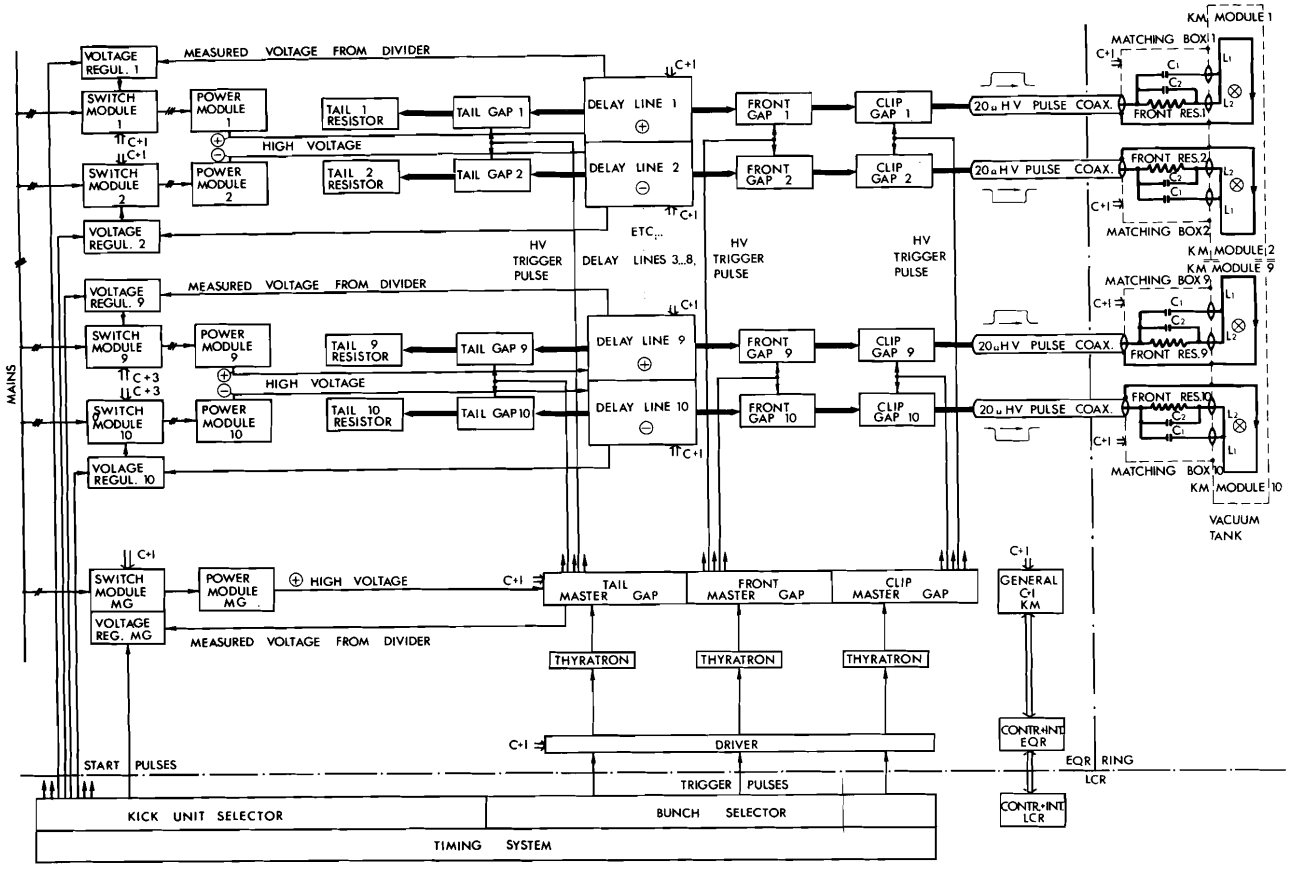

Fig. 1. Block diagram of the kicker magnet system. EQR = Equipment Room, LCR = Local Control Room, C+I = Controls and Interlocks.

switching pulse generator 1 from magnet module 1 to module 2, generator 2 to module 3, and so on. The magnet modules proper, i.e. the ferrite magnetic circuits and the excitation loops, are in the accelerator vacuum in order to minimize the aperture (Fig. 2). The terminating resistors and matching capacitors are outside the vacuum in order to minimize the vacuum requirements. This arrangement introduces additional stray inductances. Resistors and capacitors are collected in 10 identical boxes, called matching boxes, that are mounted under the vacuum tank (Fig. 3).

The delay line pulse generators have spark gap switches at both ends of the delay line. By relevant timing of the front gap (switching towards the magnet) and tail gap (switching towards a dumping resistor), the pulse duration of the kicker magnet may be varied. The long fall time of the pulse from the lumped element delay line is reduced by the clipping gap, which short-circuits the output terminals of the pulse generator.

The pulse duration is programmed for each shot on the bunch selector, which is synchronized by the timing system with the time structure of the beam in the accelerator. The bunch selector issues 3 trigger pulses for front, tail and clipping gap, that may be differently timed for each shot, depending on the particular ejection scheme. All front gaps, all tail gaps and all clipping gaps are triggered at each shot by their proper master gap, which in turn is triggered by a thyratron, driven by a hard valve pulser.

Each pulse generator is charged separately by its own HV supply, which is a transformer-rectifier set with SCR switches in its primary circuit. These switches open and start the charging process with a pulse from the timing system and stop charging when the required voltage is reached.

All pulse generators work at the same constant voltage. Shot-to-shot kick strength variation is obtained by charging only the required number of delay lines, which may be programmed on the kick unit selector. The master gap charging supply is always started. Voltage regulation is based on a zero crossing discriminator, which issues a stop pulse when the measured voltage becomes equal to a selected reference voltage.

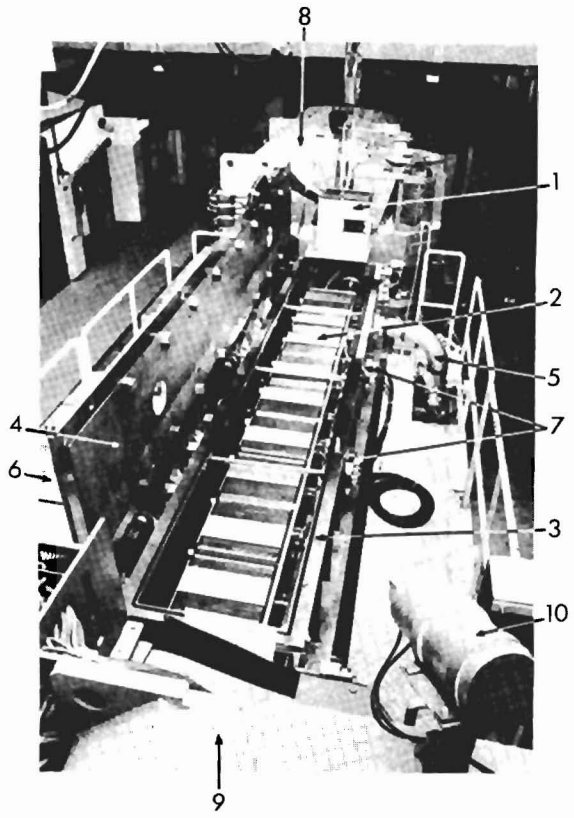

The pulses are transmitted to the kicker magnet modules through about 100 m length of coaxial HV pulse cable. Reflections from the improperly matched kicker magnet return to the latter after partial or complete reflection at the pulse generator. They may produce field variations on the flat top or spurious kicks after the main pulse. For certain pulse durations they interfere with the fall time. By choosing the cable length these reflections have been phased with the beam structure, so as to minimize the ensuing spurious deflections.

Fig. 2. View on open vacuum tank of kicker magnet inside accelerator tunnel. 1 = kicker magnet module 1, lifted out of position; 2 = modules in position; 3 = vacuum tank; 4 = tank cover; 5 = duct to turbomolecular vacuum pump; 6 = sputter ion pumps; 7 = feedthroughs for cables from field monitoring loops; 8 = upstream accelerator magnet; 9 = downstream accelerator magnet; 10= radiation monitor.

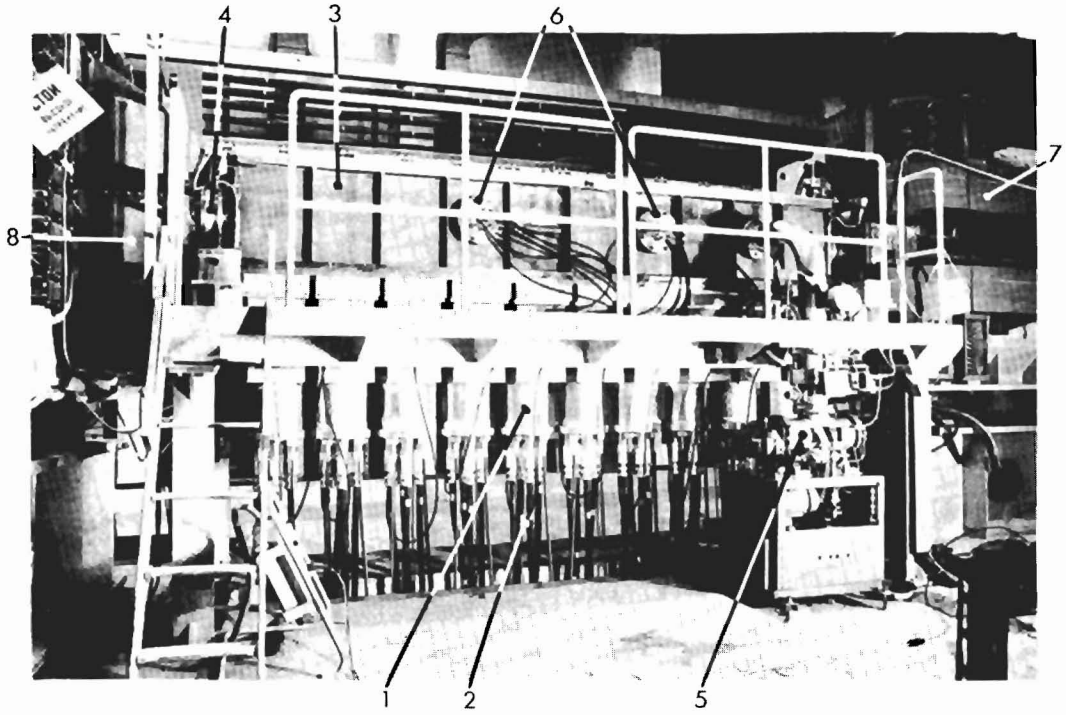

Fig. 3. Sideview on vacuum tank of kicker magnet. 1 = matching boxes; 2 = four 20 Ω pulse cables; 3 = vacuum tank; 4 = vacuum section valve; 5 = turbomolecular vacuum pump; 6 = feedthroughs for cables from field monitoring loops; 7 = upstream accelerator magnet; 8 = downstream accelerator magnet.

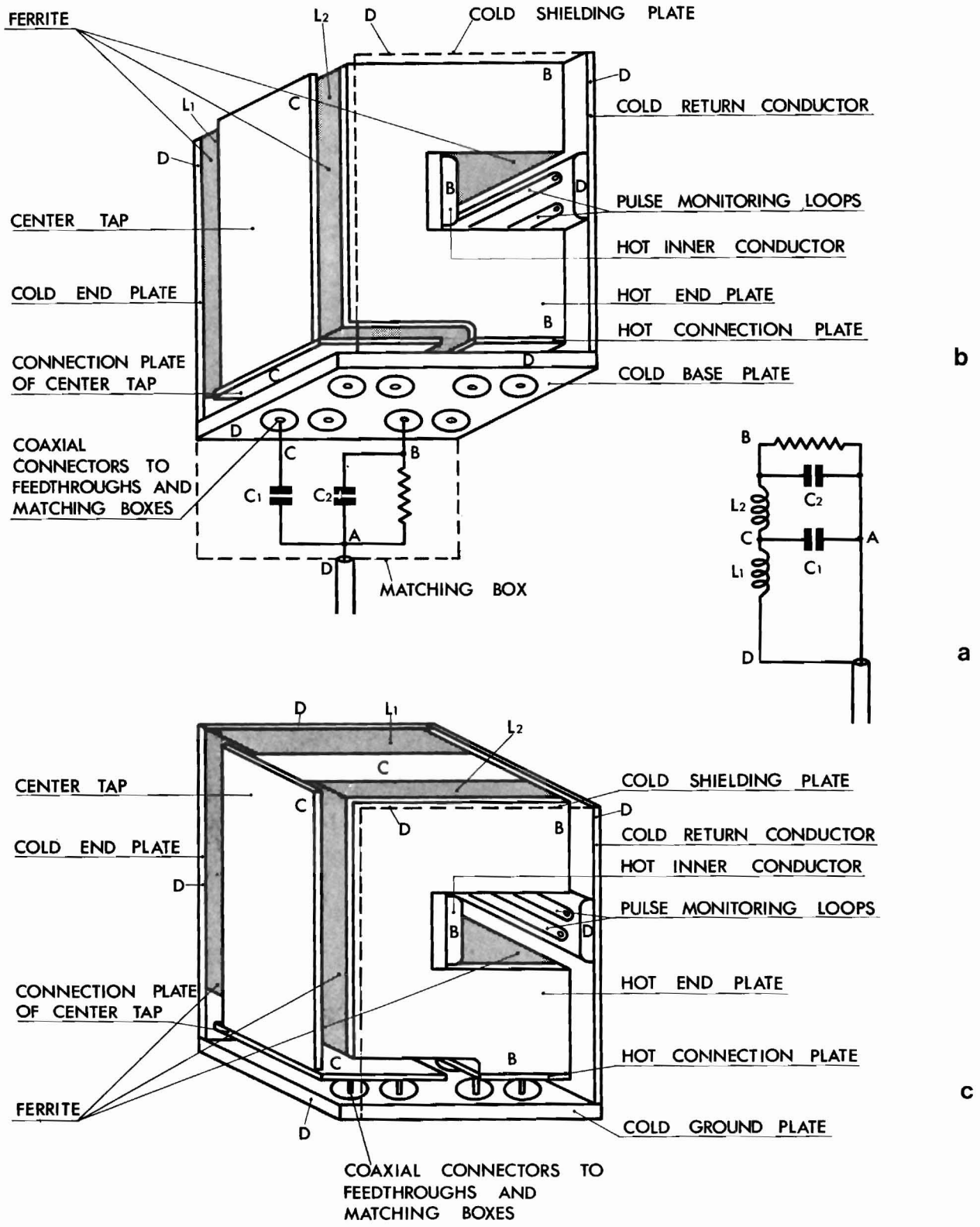

Fig. 4. a) Circuit of "Janus" kicker magnet. b) Plate covered construction of "Janus" kicker magnet; view from below. c) Plate covered construction of "Janus" kicker magnet; view from above.

III. Magnet Construction

For reasons explained in ref. 5, a two section "Janus" kicker magnet (Fig. 4a) has been made. The two inductances L_1 and L_2 are formed by two part lengths of the gap. The corresponding parts of the C-shape ferrite magnetic circuit are separated by a conductor plate, forming the centre tap C of the hot conductor. For reducing leakage fields and stray inductances, the plate covered construction of Figs 4b and 4c has been used. The engineering execution of the magnet proper, i.e. the excitation loop, the magnetic circuit, screening and connection plates, is shown in Fig. 5a and 5b. One magnet terminal is earthed; the other two go, each by a connection plate, to 4 coaxial feedthroughs in the bottom of the vacuum tank and connect to the matching capacitors and terminating resistors (Fig. 6).

The magnetic circuit is made of two sizes ferrite bricks, 200 x 130 x 28 mm^3 and 160 x 130 x 28 mm^3. There are combined into stacks with three 1 mm metal spacing discs between bricks, so as to facilitate outgassing. The stacks are kept aligned in a C-shape and pressed together by the stainless steel end plates which in turn are pulled together by traction rods going through the inner conductor.

The magnet modules stand on three vertical positioning screws and are horizontally centered by the outer conductors of the 8 pulse feedthroughs, which fit into 8 holes in the cold base plate. The modules are kept in place by their own weight and may be readily lifted out by crane after opening the vacuum tank. For this the pulse currents go from the feedthroughs to the magnet modules by coaxial beryllium bronze contact springs.

Two pulse monitoring loops are mounted on the cold conductor in the gap of each module. The upper loop permits monitoring of the individual magnetic pulses. The signals from the 10 lower loops are electrically summed, so as to yield the total magnetic kick of the magnet.

The capacitors C_1 and C_2 and the terminating resistor R are mounted in a low inductance configuration and contained in the oil filled matching box, which is mounted by four screws under the vacuum tank. Again, centering of each box is done by the outer conductors of the vacuum feedthroughs, fitting into holes of the top plate of the box. Pulse contact is made by coaxial springs. The cavities between the epoxy resin feedthroughs in the top plate of the matching box and the ceramic vacuum feedthroughs are pressurized to 3 atm with dried air. The excitation pulse enters the box at the lower side through 4 connection sockets, receiving the connector plugs of the pulse cables. There is an expansion bellows to cope with the temperature variations of the oil.

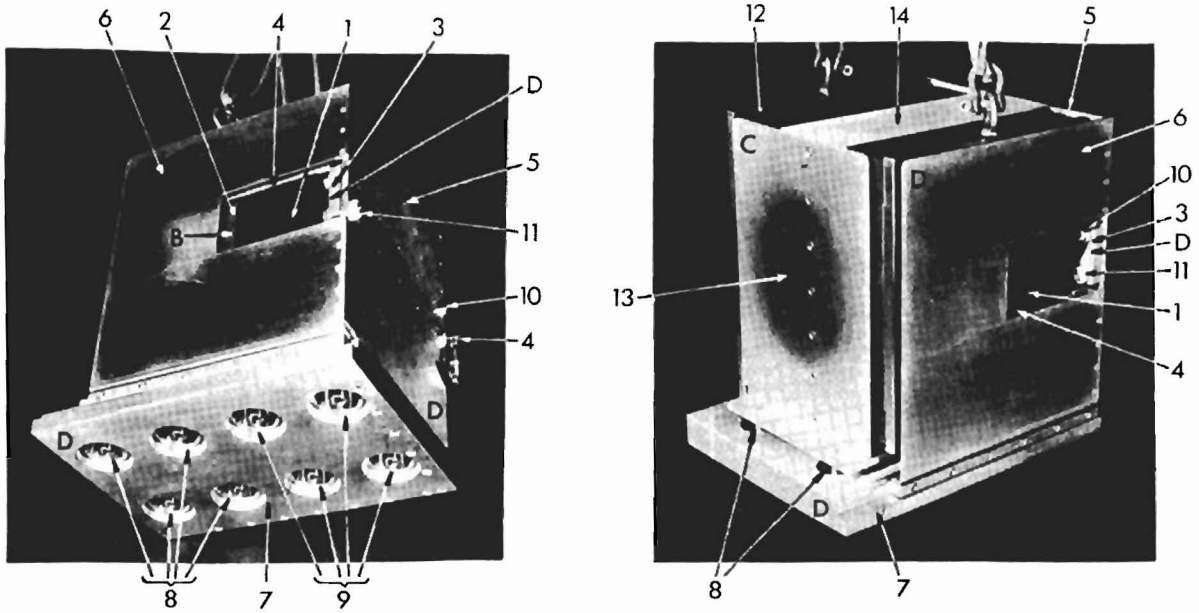

Fig. 5. Engineering execution of plate covered "Janus" kicker magnet.
a) View from below, b) view from above.
1 = Ferrite bricks inside aperture; 2 = hot inner conductor; 3 = cold outer conductor; 4 = hot front plate; 5 = cold side plate; 6 = cold shielding plate; 7 = cold base plate; 8 = coaxial connections of centre tap to C1; 9 = connections of hot conductor to C2 and R; 10 = field monitoring loop for single module; 11 = monitoring loop for sum field of 10 modules; 12 = cold back plate; 13 = hot side plate of centre tap; 14 = shield on centre tap, reducing coupling between L_1 and L_2.

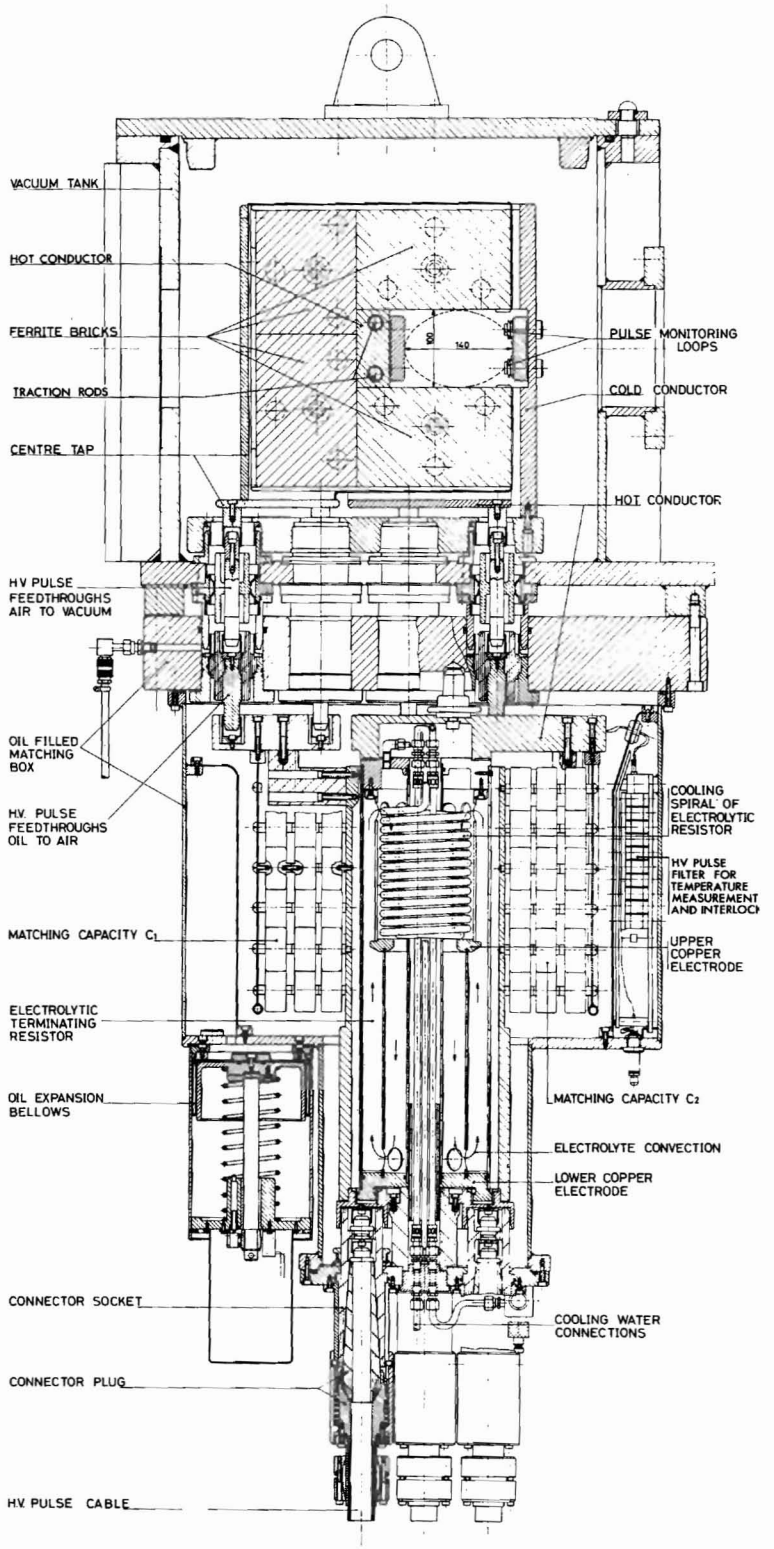

Fig. 6. Section through one kicker magnet module in vacuum tank and its matching box.

The matching capacitors C_1 and C_2 consist of series-parallel clusters of HV ceramic capacitors.

The terminating resistor R has a $CuSO_4$ electrolytic solution between copper electrodes. The dissipated power is removed by cooling water flowing through a spiral in the electrolyte. This spiral is "hidden" behind the upper current electrode, so that erosion of the spiral is negligible. The resistance is temperature dependent and the temperature is stabilized at 40°C. The temperature control system sends alternatively cold and hot water through the spiral. Hot water is predominantly used at small pulse durations and repetition rates, where heat losses exceed dissipated power. There are temperature sensors going into the electrolyte through the upper electrode. A balanced HV filter in the leads of the temperature sensors reduces the 50 kV common mode surges from the upper electrode to levels acceptable for the solid state electronics of the temperature control system.

IV. Performance

The magnet performance came out close to predictions.

Figure 7 gives the kick of one isolated module as a function of the excitation current and line voltage. At field levels of B = 0.1 T, the permeability of the ferrite is $\mu_r \simeq 1000$. The homogeneous part of the field in the centre of the gap is therefore given by the excitation current and gap height, within 1 % error. For

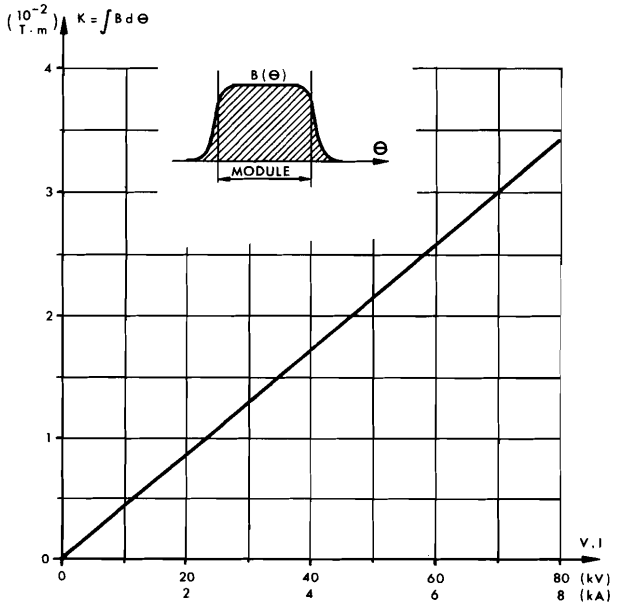

Fig. 7. Magnetization curve for one isolated module; kick K, as measured with a long coil embracing leakage fields, as a function of line voltage V and excitation current I with a circuit matched to 5 Ω .

an excitation current of 8 kA, one finds B = 0.1 T. For the same current the kick is found to be K_1 = 0.034 T·m, so that the magnetic length of one isolated module, where the leakage flux is free to fan out, becomes ℓ_{m1} = 0.34 m. When the modules are placed in tandem in the tank, this may be slightly less. Due to difficulties in measuring the large fast current pulse, the error may be up to 5 %.

The kick variation in the median plane is less than the relative measuring precision of ± 1 % over a radial width of ± 50 mm around the centre of the aperture.

Figure 8 shows a number of typical oscillogrammes of the time variation of the magnetic kick of one of the 10 modules in the vacuum tank. On some of them the proton bunch structure of the circulating beam gives a time mark of 165 nsec interval. These bunches are not necessarily optimally phased with the pulses shown. One discerns the reflections, the length of which permits phasing them between passage of proton bunches, hence keeping spurious beam deflections small.

The remanent field has been measured after repeated excitation with 8 kA pulses of 5 μsec duration, i.e. to a field of B = 0.1 T. The levels found are roughly consistent with estimations based on the corresponding coercive force of H_c = 0.33 Oe and the magnet geometry. Figure 9 shows the longitudinal variation on the centre line of the gap. The levels found for the 10 modules varied by ± 20 % around their average value, but their quadrupole component is approximately equal. Figure 10 gives the radial variation of the total remanent kick of the 10 modules in the median plane and in parallel planes at ± 35 mm distance.

During a number of test sessions the magnet was exercised through most of its applications in the accelerator and the proton beam behaved as expected.

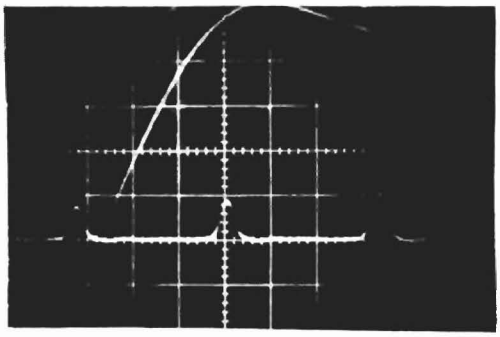

a

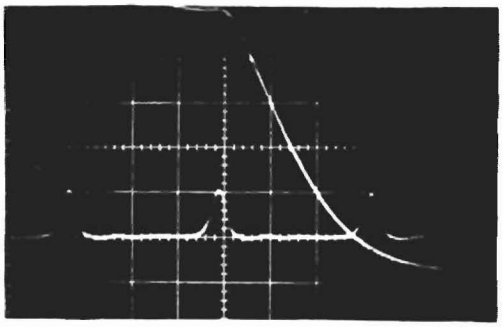

b

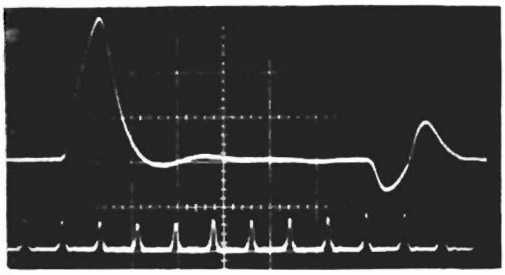

c

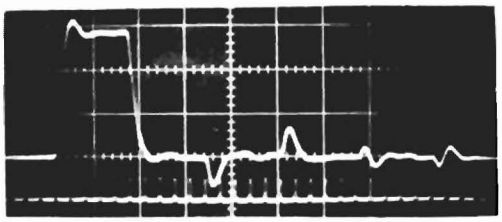

d

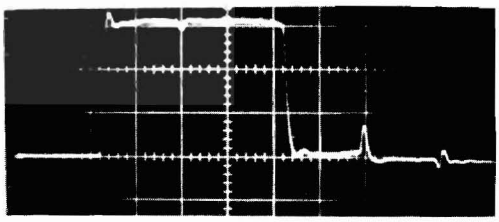

e

Fig. 8. Typical time variation of the kick of one of 10 modules in vacuum tank. Second trace: bunch structure of proton beam. Bunches at 165 ns interval but not optimally phased with rise and fall of pulses. Reflections occur either after 1.65 μsec, i.e. 10 bunch intervals (d and e, before cutting cables to length) or after 1.32 μsec, i.e. 8 bunch intervals (c, after cable cutting).

a) Rise time of pulse for 2-bunch extraction; 50 nsec/div.

b) Fall time; 50 nsec/div.

c) Pulse and reflection for single bunch extraction of rise and fall superimposed; 200 nsec/div.

d) Pulse for 5-bunch extraction with first reflections of rise and fall, thereafter second reflections; 500 nsec/div.

e) Pulse for 24-bunch extraction with first (partial) reflection of rise on flat top and first and second reflections of fall; 1 μsec/div.

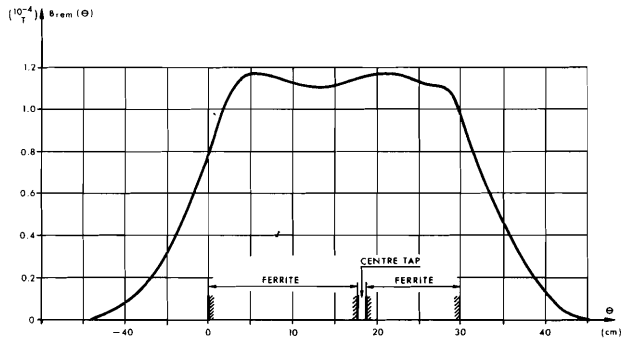

Fig. 9. Remanent field B_{rem} of centre line of gap of one isolated module as a function of azimuth Θ; obtained from a Hall probe scan, after repeated excitation with 8 kA pulses of 5 μsec duration.

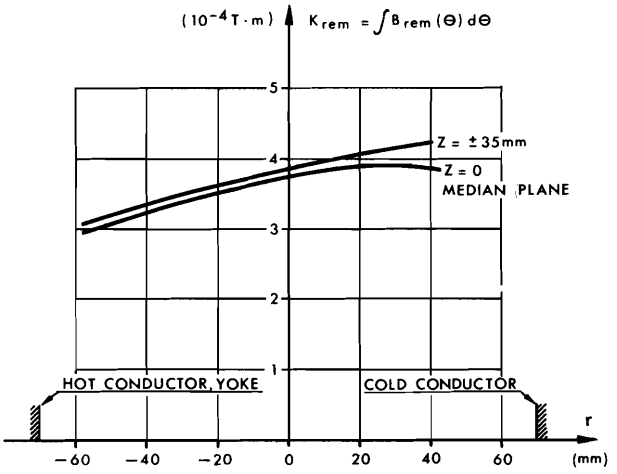

Fig. 10. Total remanent kick K_{rem} for 10 modules as a function of the radial position r. Obtained by summing of long coil measurements on the 10 isolated modules after repeated excitation with 8 kA pulses of 5 μsec duration.

Acknowledgements

It is a pleasure to thank Y. Favereau for mechanical design and construction of all prototypes and B. Féral for his intelligent assembly and adjustment of the final magnets. We are also indebted to R. Bonvin and J. Hofmann for their competent electrical work on the kicker magnet system.

References

1. G.K. O'Neill and V. Korenman, The Delay Line Inflector, Princeton Pennsylvania Accelerator Project, Report GKON 10, VK 13, (Dec. 1957).

2. E.B. Forsyth and M. Fruitman, Fast Kickers, Particle Accelerators 1, p. 27 (1970).

3. B. Kuiper, B. Langeseth and K.P. Myznikov, The Fast Ejection System, in particular Channel A, of the Serpukhov Accelerator, Proc. Intern. Conf. on High En. Accelerat., vol. 1, p. 549, Yerevan, 1969.

4. R. Bossart et al, Multishot and Multichannel Fast Ejection, IEEE Trans. Nucl. Sci. NS-16 N° 3, 286 (1969); also R. Bossart et al, Multiple Shot and Multiple Channel Operation of the CPS Fast Ejection System, Proc. Int. Conf. on High-En. Acc., vol. 1, p. 624, Yerevan, 1969.

5. P.G. Innocenti, B. Kuiper, A. Messina, H. Riege, On the Design of "Fast Kicker" Magnets, presented at the 3rd Inter. Conf. on Magnet Technology, Hamburg, 1970, p. 559.

6. B. Kuiper and G. Plass, On the Fast Extraction of Particles from a 25 GeV Proton Synchrotron, CERN 59-30.

7. R. Bossart et al, The Fast Ejection Equipment for the Serpukhov 70 GeV Proton Synchrotron. Proc. 8th Int. Conf. High En. Acc., p. 116, CERN 1971.